Egyptian Knowledge Bank
https://ijmti.journals.ekb.eg/

International Journal of Materials Technology and Innovation
Volume 2, Issue 1 (2022), pages 35-50

Online ISSN 2682-4299

Synthesis of High Hardness Hydroxyapatite Particles using Surfactant Assisted Hydrothermal Method

***E. A. Abdel-Aal, H. M. Abdel-Ghafar, D. El-Sayed, E. M. Ewais.**

Central Metallurgical Research and Development Institute (CMRDI), P.O. Box 87 Helwan, Cairo, Egypt

*Corresponding author: E-mail: eabde2@gmail.com

Received 13 January 2022
Revised 23 March 2022
Accepted for publication 16 June 2022
Published online 17 June 2022

Abstract

Hydroxyapatite (HA) crystals were synthesized from calcium acetate monohydrate and phosphoric acid using hydrothermal method. The various interactions of reactant concentrations (1 – 3 Molar), surfactant {aminotris (methylene phosphonic acid) $[N(CH_2PO_3H_2)_3]$ (ATMP)} concentrations (0 - 100 ppm), and hydrothermal times (6 – 24 hours) were investigated and their effects on the mean diameter of the HA crystals were obtained using the Box-Behnken experimental statistical design. Results have shown that surfactant has no effect on the mean diameter of the crystals. On the other hand, the results revealed that time and reactant concentration are major parameters in changing the particle size of hydroxyapatite crystals. Without addition of the surfactant, well elongated crystals with high degree of crystallinity were synthesized. With addition of the surfactant, the agglomeration of HA particles as well as hardness of HA pressed discs are significantly increased. HA particles were ranged from 2.7 µm to 7.2 µm as crystal aggregates whereas the obtained crystallite sizes ranged from 17.3 nm to 30.3 nm.

Highlights

- The paper involves new findings on the synthesis of high hardness hydroxyapatite.
- 15 synthesis tests via experimental statistical design were performed with discussion of the results.
- Investigations of hydroxyapatite with and without the ATNP surfactant are reported.
- The hydroxyapatite hardness is increased with the addition of surfactant.

Graphical Abstract

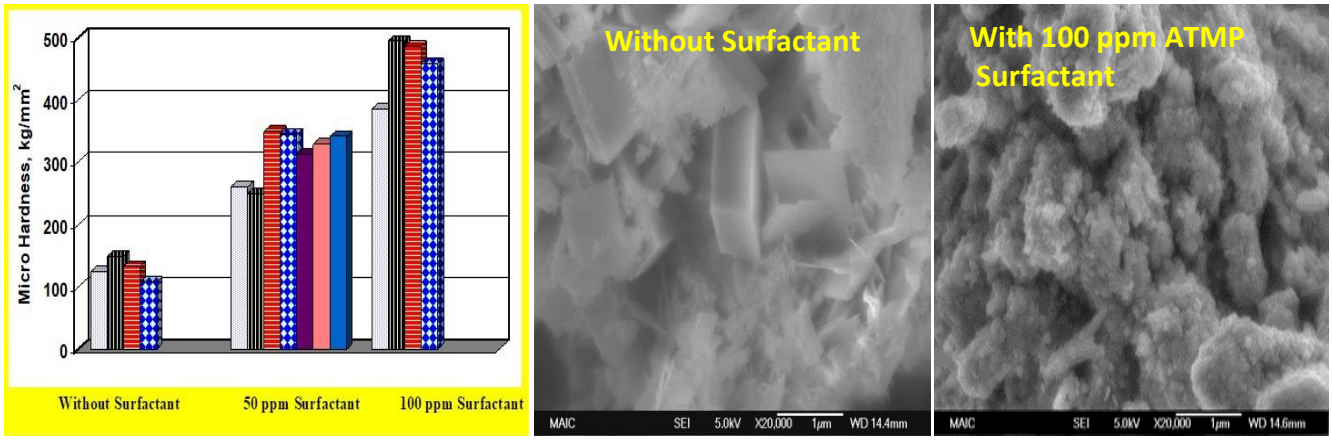

Keywords: Biomaterials; Chemical synthesis; Crystallization; Hardness.

IJMTI vol. 2, issue 1 (2022) 35-50 https://doi.org/ 10.21608/ijmti.2022.115060.1044

1. Introduction

Hydroxyapatite (HA) is a complex salt of calcium and phosphorous with a stoichiometric composition of $Ca_{10}(PO_4)_6(OH)_2$ with a calcium to phosphorous ratio of 1.667. It has been studied intensively because of its presence in hard tissue materials such as the matrix of the bones, tooth dentin, and enamel. Usually, the HA content in the human body is around 65% [1]. Hydroxyapatite is important for its use in the biomedical field for artificial bone grafting because of its open porosity. Open porous HA allows a fast build-up of tissues and good osteoconduction. However, dense synthetic hydroxyapatite ceramic powders have exhibited low fracture toughness when compared with the values of human bones. Hydroxyapatite whiskers have generally exhibited high tensile properties because of their low dislocation density. With this view, needle-like crystals of hydroxyapatite have been synthesized for improving fracture toughness [2 - 5].

The general methods of HA synthesis include hydrothermal method [3, 6,7], solid-state reaction [8], precipitation [9-11], sol-gel [12, 13], sputtering [14], mechanochemical [15, 16], mechanochemical–hydrothermal [17], electrodeposition (electrocrystallization) [18-22], microemulsion [23] and others. Hydrothermal technique has the advantage of controlling the size of precipitating material by controlling supersaturation [245 24]. Poly(sodium 4-styrene-sulfonate) (PSS) was used as an organic template to induce the formation of hydroxyapatite with different morphologies prepared by the hydrothermal method [26]. Long and uniform HA whiskers with high crystallinity (mean length of 60–116 μm), controlled morphology, and high aspect ratio of 68–103 were synthesized by hydrothermal homogeneous precipitation using acetamide, calcium nitrate and diammonium phosphate with initial pH of 3.0 [27]. Addition of amino tris(methylenephosphonic acid) [ATMP] surfactant for gypsum crystallization was studied [28]. It was found that this surfactant decreased the crystal growth rate, mean diameter, the free energy for the formation of critical nucleus size, and the radius of critical nucleus, whereas the nucleation rate increased [28]. Macromolecules such as stearic acid, monosaccharides, and related molecules are added during HA preparation to control its morphology [29].

The present investigation aimed to explore the effect of amino tris(methylenephosphonic acid) surfactant on HA morphology under hydrothermal conditions (i.e. at 140 °C) from phosphoric acid and calcium acetate monohydrate and to identify the optimum HA preparation conditions using Box Behnken experimental statistical design. Knowing that ATMP surfactant inhibits the crystallization of calcium sulfate dihydrate in an acidic medium, so, this research will explore the effect of ATMP on hydroxyapatite but at an alkaline pH of 9.0.

2. Materials and Methods

2.1. Hydrothermal synthesis

The Box Behnken design was used to develop an experimental procedure that would identify the main effects of varying factors (Table 1). From this data, optimal conditions could be obtained and conclusions based on statistical significance could be drawn. For these experiments hydrothermal time, concentration of reactants, and concentration of surfactant were varied throughout 15 experiments.

The reactants used were phosphoric acid and calcium acetate monohydrate from Fisher Company of 99.9% purity. They were added in stoichiometric amounts according to the following reaction:

$$6H_3PO_4 + 10Ca(C_2H_3O_2)_2.H_2O \longrightarrow Ca_{10}(PO_4)_6(OH)_2 + 20CH_3COOH + 8H_2O \quad (1)$$

According to the Box Behnken design in Table 1, the desired amounts of distilled water and surfactant were added to the reactor. The surfactant used was amino tris (methylenephosphonic acid) $[N(CH_2PO_3H_2)_3]$ from Pfaltz & Bauer Incorporation (ATMP) of 0.18 % and has another name as Nitrilotrimethylphosphonic acid (amino tris). The purity of ATMP is 99.8 5%. Phosphoric acid of 99.9% purity and calcium acetate monohydrate were reacted in a Ca/P ratio of 1.667 without or with 50 ppm or 100 ppm of surfactant (Table 1).

The calculated amounts of phosphoric acid and calcium acetate solutions were added to the reactor and allowed for one hour of reaction time with agitation. The resulting mixture was acidic (pH ranged from 2.4 to 3.4). After mixing for 1 hour, the solution was then adjusted to pH 9.0 $\pm$ 0.1 using ammonium hydroxide. This pH is the optimum pH for precipitation of hydroxyapatite owing to its very low solubility at this pH. The mixture was then placed in a pressure vessel (half-filled) and put in the oven for the required time ranging from 6 hours to 24 hours at a constant temperature of 140 °C. After, hydrothermal time, the resulting mixture was naturally cooled, filtered, and washed.

IJMTI vol. 2, issue 1 (2022) 35-50 https://doi.org/ 10.21608/ijmti.2022.115060.1044

Table 1 Conditions and Results of the 15 Tests of Experimental Design.

Test No.	Coded Factor Levels			Mean Diameter, µm	Crystallite size, nm	Micro hardness, kg/mm^2
	Time, hr.	Concentration, M	Surfactant, ppm			
1	6	1	50	3.7	23.1	261
2	6	3	50	7.2	20.6	250
3	24	1	50	3.1	22.0	350
4	24	3	50	5.3	21.9	345
5	6	2	0	2.9	23.1	124
6	6	2	100	2.7	30.3	385
7	24	2	0	5.0	23.0	149
8	24	2	100	5.1	23.0	494
9	15	1	0	4.2	19.6	133
10	15	1	100	3.8	22.8	486
11	15	3	0	4.6	20.3	108
12	15	3	100	4.3	17.3	458
13	15	2	50	3.1	22.8	313
14	15	2	50	3.3	20.4	330
15	15	2	50	3.5	22.0	341

The precipitated hydroxyapatite was dried at a temperature of 60 °C for 24 hours. The dried samples were ground in a mortar to obtain fine crystals of hydroxyapatite, which are then pressed with a 25 mm die (ICL, Macro/ Micro KBr Die) used for isostatic pressing. The die is pre-lubricated with 1-2 drops of oleic acid and the obtained pellets are calcined and sintered. Sintering procedure was as the following:

- Temperature was increased from room temperature to 800 °C at a rate of 2 °C per minute and maintained at 800 °C for 2 hours.
- Temperature is then raised from 800 °C to 900 °C at a rate of 2 °C per minute and maintained at 900 °C for 1 hour.
- Temperature is then raised from 900 °C to 1200 °C at a rate of 2 °C per minute and maintained at 1200 °C for 1 hour.
- Finally, the temperature is then naturally decreased from 1200 °C to room temperature.

2.2. Particle size distribution

Laser light scattering technique (Coulter LS 230, Beckman Coulter Corp., Miami, Fl) was utilized to identify the particle size distribution of the samples obtained. Samples were taken from a slurry of each Test. Each sample consisted of 8 mL of slurry dispersed in 50 ml of distilled water. All samples were then sonicated for 45 minutes and kept under constant agitation immediately before analysis. Then, the sample was poured inside the chamber of the Coulter instrument after flushing three times with distilled water.

IJMTI vol. 2, issue 1 (2022) 35-50 https://doi.org/ 10.21608/ijmti.2022.115060.1044

2.3. Microstructure characterization

Hydroxyapatite samples were subjected to different characterization using X-ray diffraction analysis (BRUKER X-Ray Diffractometer), Crystallite size (L_c) of the hydroxyapatite phase was calculated using Scherrer's Equation No. 2:

$$L_C = \frac{k\lambda}{\beta \cos\theta} \quad (2)$$

Where: k is the shape coefficient, λ is the wavelength, β is the full width at half maximum (FWHM) of each phase, and θ is the diffraction angle [15]. The hydroxyapatite particles were characterized by Scanning Electron Microscopy SEM (LEO 1455VP). Transmission Electron Microscope (TEM, JEOL-JM1230) was used for observation of the particle's morphology.

2.4. Hardness measurement

Vickers hardness of the obtained HA material is conducted after pressing and sintering the pellets. All the pellets were subjected to a Vickers microhardness tester (Micromet 3, Buehler LTD., Lake Bluff, IL). The pellets were indented on their polished surfaces. The Vicker's hardness of the pellets (H_V) was calculated according to Equation (3), where, L is the indentation load in Newtons, 2a, the average diagonal length of the indentation in meters [30]. From 5 to 8 indentations were done on each specimen using a load of 1 kilogram with a 10-second loading time. Then average hardness value for each pellet was calculated.

$$H_V = L/2a^2 \quad (3)$$

2.5. Statistical experimental design tests

The obtained results of the 15 Tests of the experimental statistical Box–Behnken design with their experimental conditions are given in Table (1). The statistical Box–Behnken design program was applied to the obtained results. The resulting graphs are presented and discussed below showing general trends illustrating the most significant factors affecting the microhardness and the mean diameter of HA particles.

3. Results and Discussion

3.1. Effect of hydrothermal time and reactants concentration on HA microhardness

Fig. 1 shows the effects of hydrothermal time and concentration of reactants using different surfactant concentrations (0, 50, and 100 ppm) on the micro hardness of precipitated HA. From these results, it can be seen that, with increasing the hydrothermal reaction time, the HA microhardness was very slightly decreased at all the levels of surfactant concentrations. Moreover, with increasing the concentration of the reactants, the HA micro hardness did not have gain pronounced changes at all hydrothermal times.

3.2. Effect of hydrothermal time and surfactant concentration on HA microhardness

Fig. 2 illustrates the effects of hydrothermal reaction time and surfactant concentrations using different reactant concentrations (1 M, 2 M, and 3 M H_3PO_4) on the micro hardness of precipitated HA. The highest hardness of all the HA samples was obtained at a high surfactant concentration of 100 ppm and at the shortest reaction time of 6 hr.

3.3. Effect of reactant and surfactant concentrations on HA microhardness

Fig. 3 illustrates the effects of the reactant and the surfactant concentrations at different hydrothermal reaction times (6, 15, and 24 hr.) on the micro hardness of precipitated HA. The highest hardness of all HA particles was obtained at the highest concentration of surfactant.

Phosphoric acid concentration does not affect the microhardness of HA crystals.

3.4. Effect of synthesis conditions on HA microhardness and mean diameter

All the experimental data with microhardness response are collected at the 3-D cubic and are given in Fig 4. This cubic diagram shows that the highest microhardness of about 397 to 537 Kg/mm^2 was achieved at a high level of surfactant concentration (100 ppm) at any level of other conditions.

Also, all the experimental data with mean diameter response are collected at the 3-D cubic and are given in Fig. 5. This cubic diagram shows that a mean diameter of about 7.1 to 7.3 microns could be achieved at a high level of reactants concentration (3 M H_3PO_4), low level of hydrothermal time (6 hr), and with or without the addition of surfactant. With increasing reactant concentration, the HA mean diameter was increased. On the other hand, with increasing hydrothermal time, the HA mean diameter was decreased. The smallest mean diameter (3.09 – 3.14 microns) can be obtained at a low level of

IJMTI vol. 2, issue 1 (2022) 35-50 https://doi.org/ 10.21608/ijmti.2022.115060.1044

reactant concentration (1 M H_3PO_4) and a high level of hydrothermal time (24 hr) with or without surfactant.

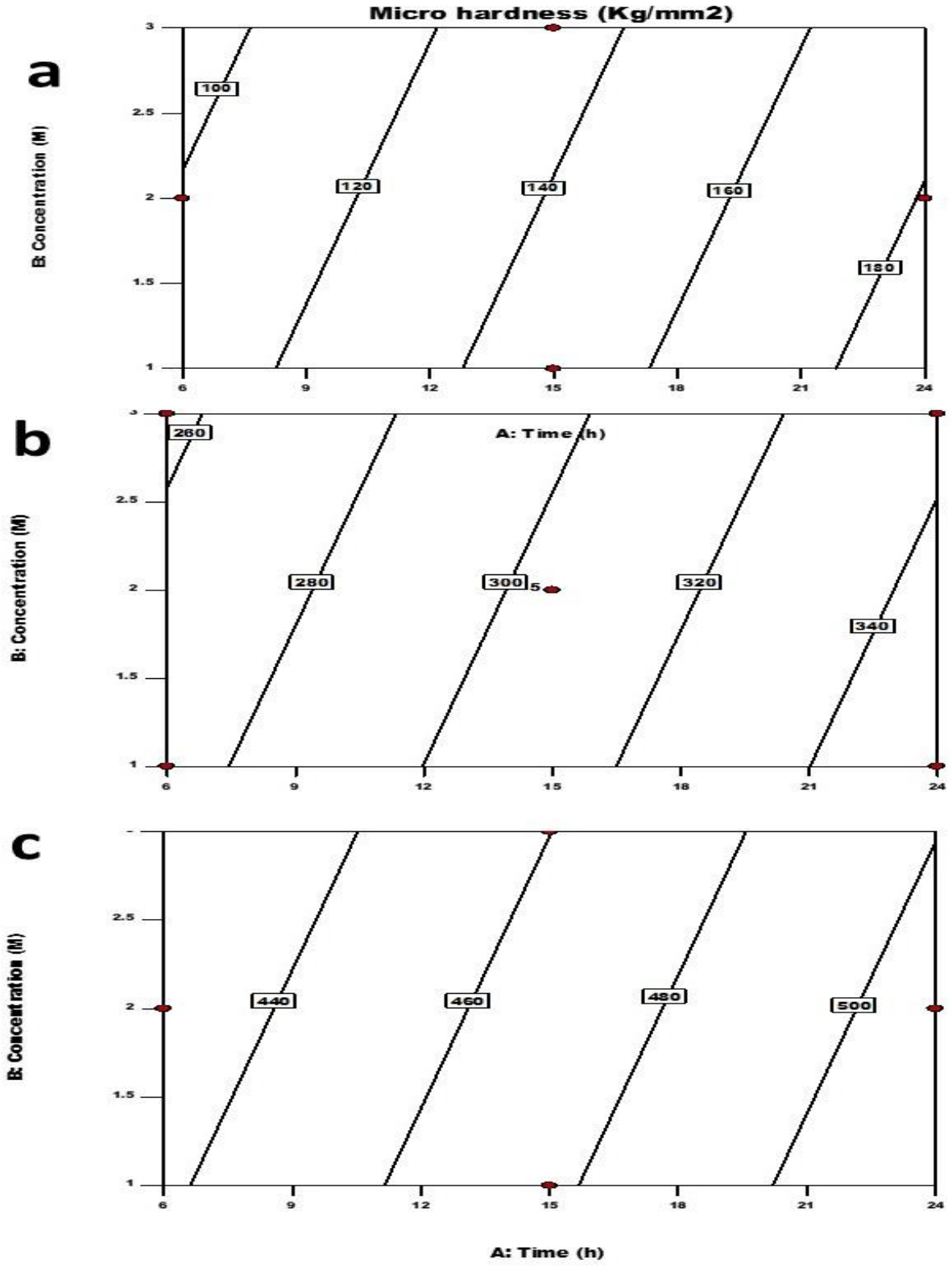

Fig. 1 Effect of Hydrothermal Time and Reactants Concentration on HA MicroHardness at Different Surfactant Concentrations 0 ppm(a); 50 ppm(b); 100 ppm(c).

IJMTI vol. 2, issue 1 (2022) 35-50 https://doi.org/ 10.21608/ijmti.2022.115060.1044

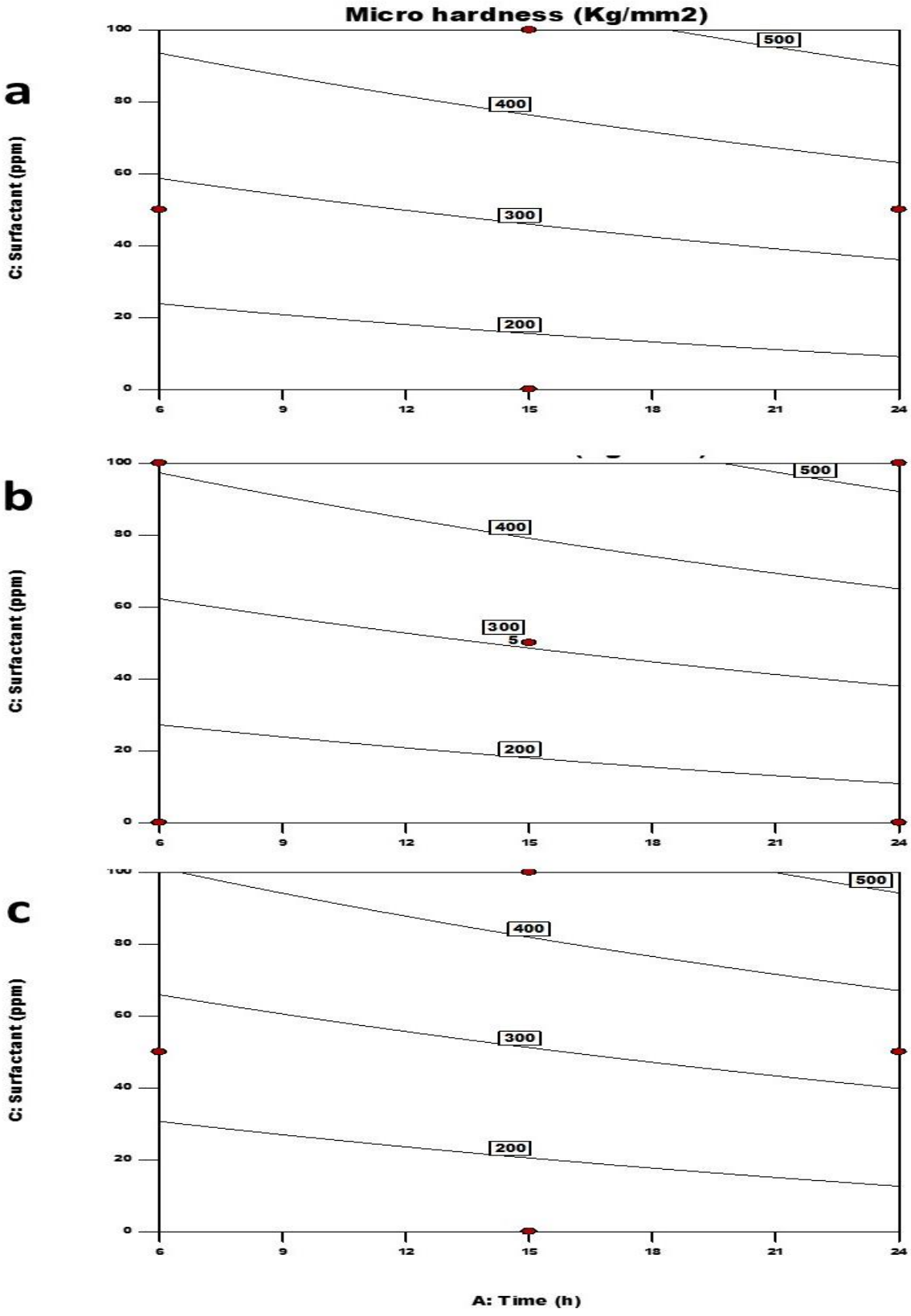

Fig. 2 Effect of Hydrothermal Time and Surfactant Concentration on HA Micro Hardness at Different Reactant Concentrations; 1M (a), 2M (b), and 3M (c)

IJMTI vol. 2, issue 1 (2022) 35-50 https://doi.org/ 10.21608/ijmti.2022.115060.1044

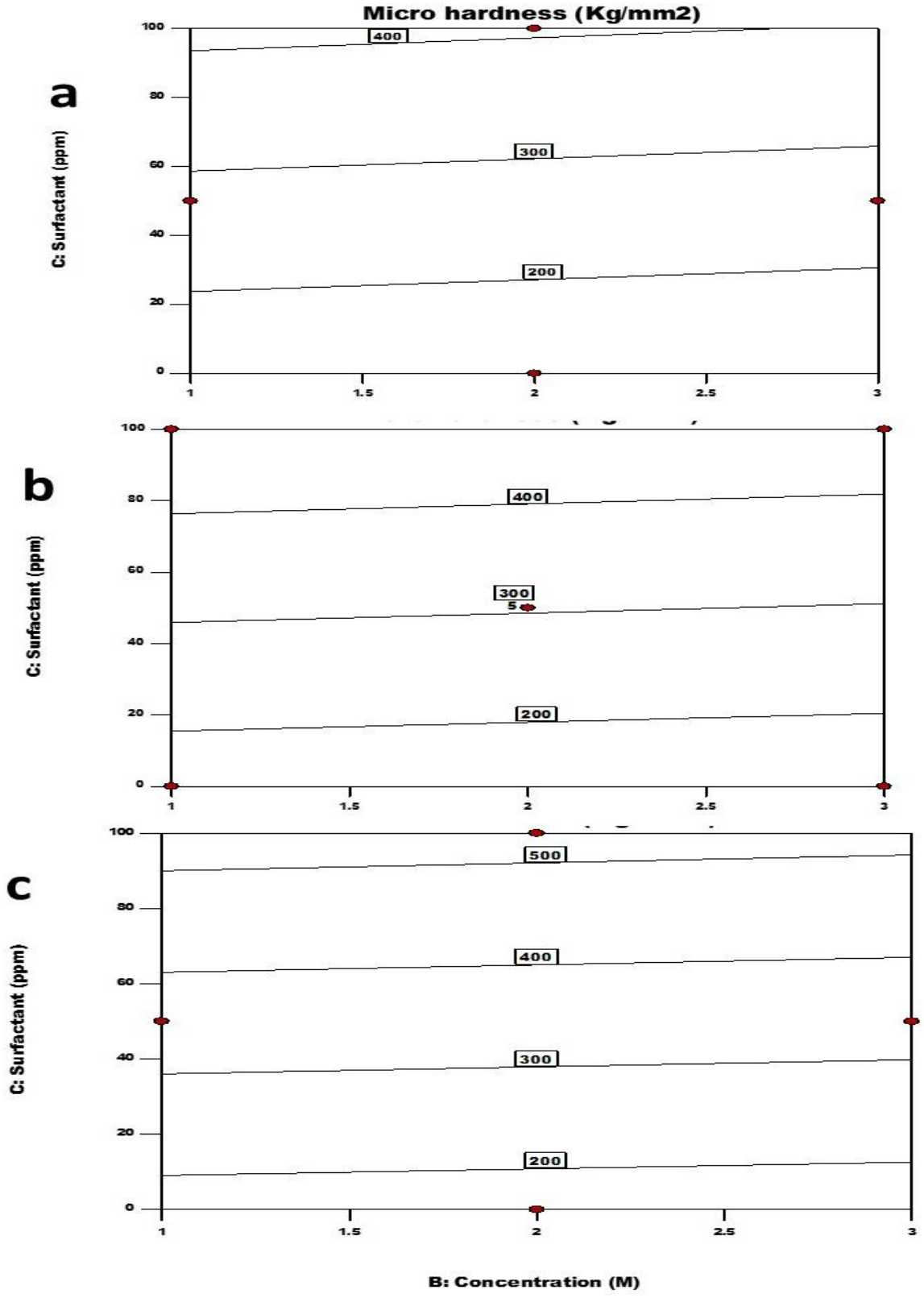

Fig. 3 Effect of Reactant and Surfactant Concentrations on HA Micro Hardness at Different Hydrothermal Times; 6h (a), 15h (b), and 24h (c)

IJMTI vol. 2, issue 1 (2022) 35-50 https://doi.org/ 10.21608/ijmti.2022.115060.1044

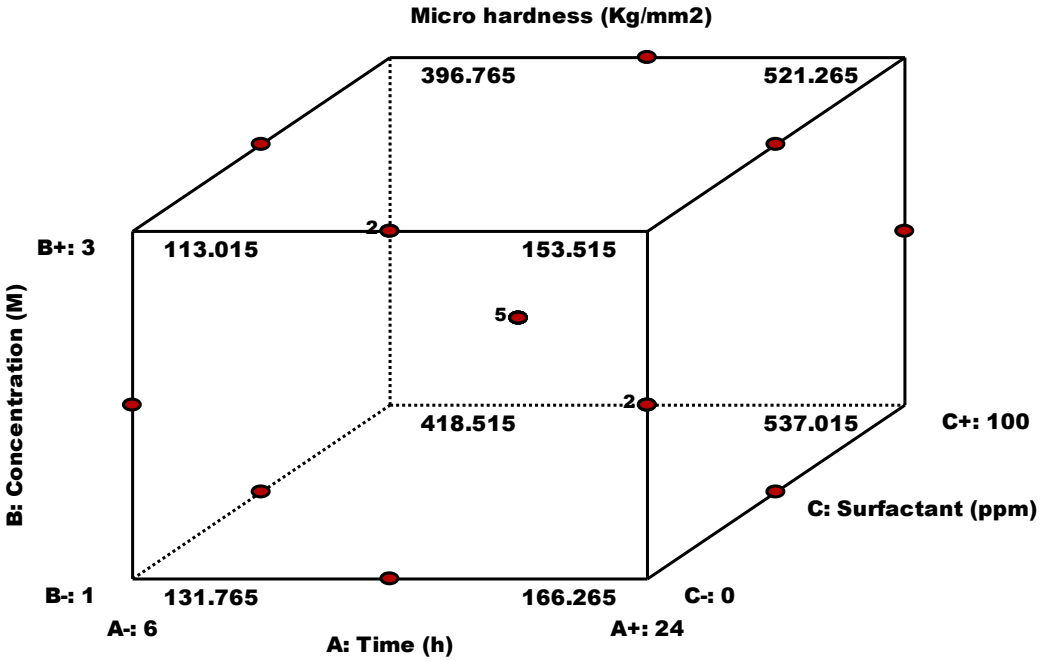

Fig. 4 3-D Plot for the Experimental Data.

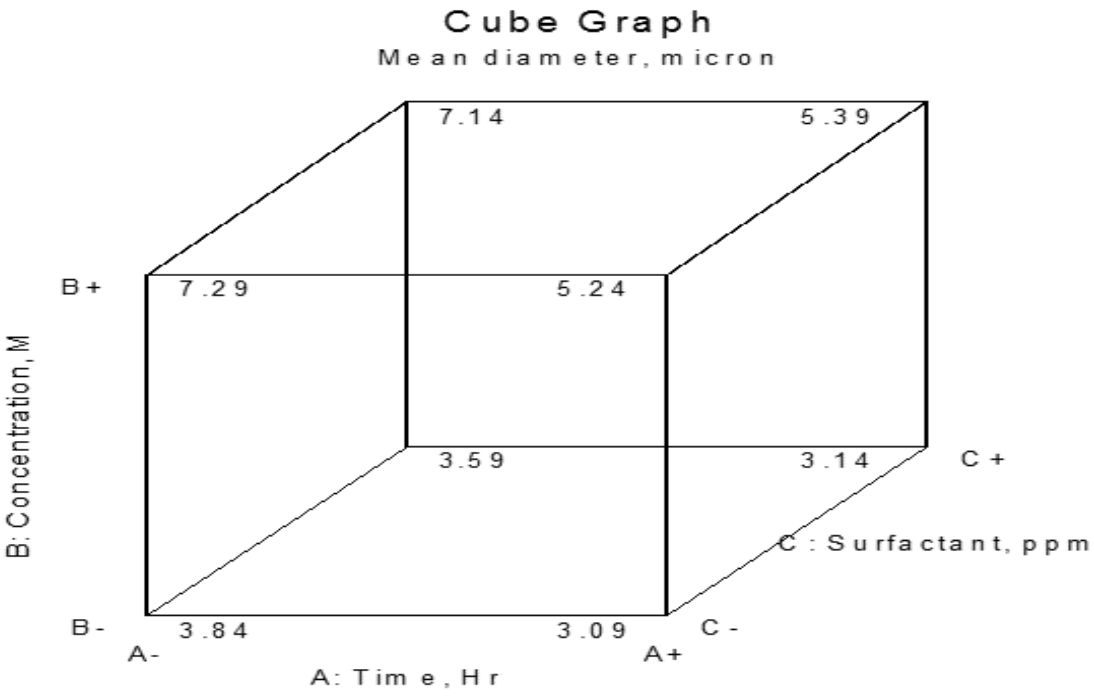

Fig. 5 3-D Plot for the Experimental Data.

IJMTI vol. 2, issue 1 (2022) 35-50 https://doi.org/ 10.21608/ijmti.2022.115060.1044

3.5. Effect of surfactant concentration and mean diameter on HA hardness

The effect of amino tris(methylenephosphonic acid) surfactant concentrations on hydroxyapatite hardness is given in Fig. 6. It is interesting that, with increasing surfactant doses, the HA hardness was increased whatever the other conditions. It is worth mentioning that, the hardness of human bone is 50 kg/mm^2 [31]. The obtained hardness values ranged from 108 to 494 kg/mm^2 which are higher than human bone hardness. The suggested mechanism for increasing the hardness by adding this surfactant is the formation of agglomerated nanoparticles which after sintering give high hardness and high shrinkage. On the other hand, tabular HA crystals will form without surfactant which gives low hardness. These findings are discussed in detail in item 3.8.

Particle size distribution was done for all the HA samples. Fig. 7 shows the particle size distribution of 5 samples (Tests 1 to 5). The mean diameter of the samples ranged from 2.7 µm to 7.2 µm (Table 1).

No correlation was found between HA mean diameter and hardness as shown in Fig. (8).

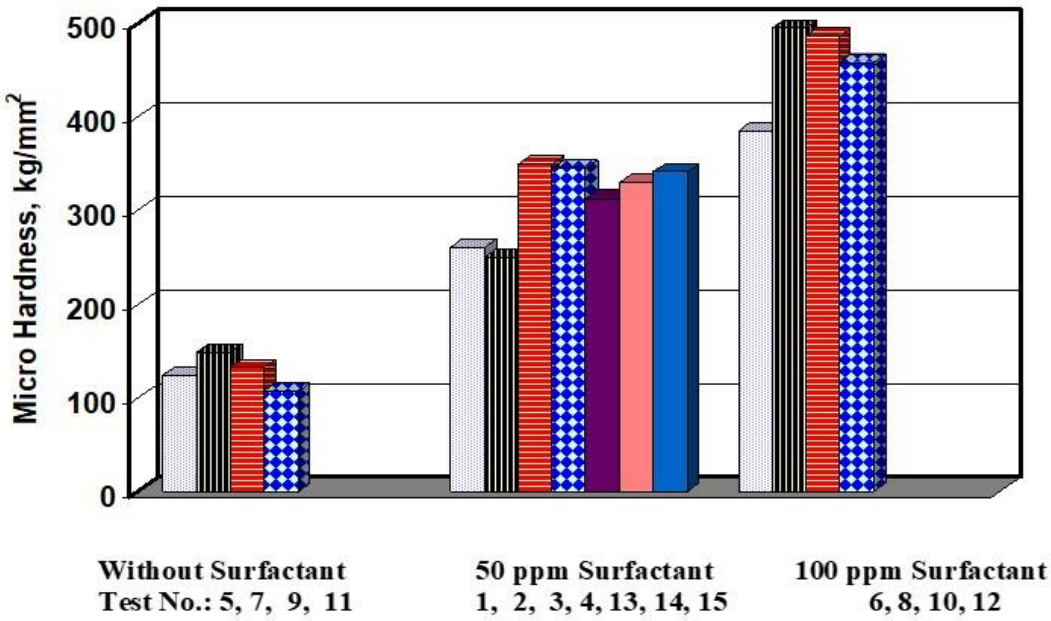

Fig. 6 Effect of Surfactant on Hydroxyapatite Hardness.

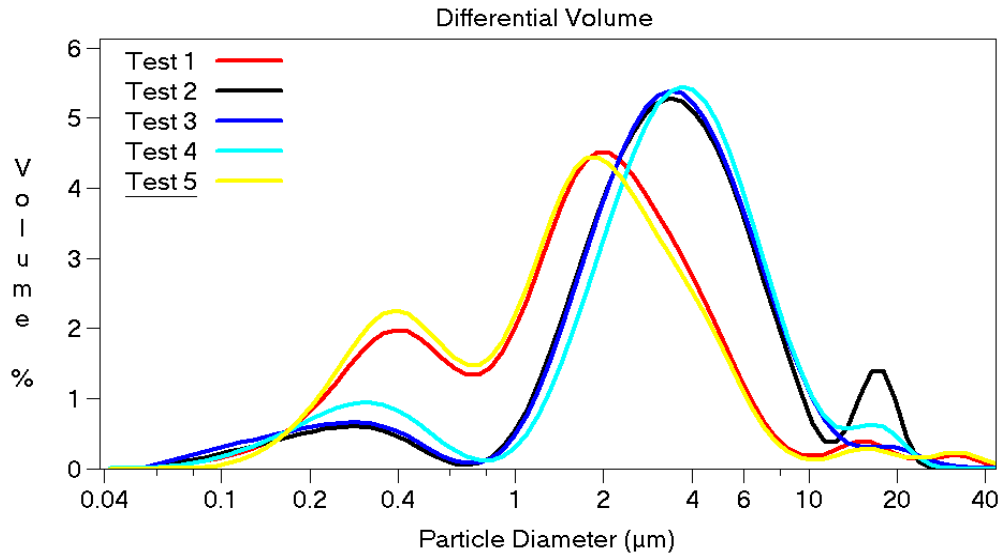

Fig. 7 Crystal Size Distribution of Hydroxyapatite Powders (Tests 1-5).

IJMTI vol. 2, issue 1 (2022) 35-50 https://doi.org/ 10.21608/ijmti.2022.115060.1044

3.6. Characterization of crystallized HA powder

The precipitated powder was characterized using XRD, SEM, TEM, and Laser Size Distribution. X-ray diffraction pattern (Fig. 9) was conducted on the 15 samples. The precipitated phase was confirmed as hydroxyapatite [JCPDS # 00-009-0432]. The crystallite size ranged from 17.3 to 30.3 nm as shown in Table (1). The intensity of peaks at 2 Theta of 26 is increased from samples numbers 13, 14, and 15 (similar medium conditions) to sample number 12 (high reactant concentration with 100 ppm surfactant) to sample number 11 (high reactant concentration without surfactant) as shown in Fig. 9.

Fig. 10 shows SEM photomicrographs of the crystallized hydroxyapatite powder samples (Tests 1 – 4, 7, and 8). It is clear that the crystallized hydroxyapatite powders from all the Tests are agglomerated particles of different sizes. However, increasing reactant concentration (Tests 2 and 4) gave larger agglomerated particles compared with low concentration (Tests 1 and 3). To understand the effect of amino tris(methylenephosphonic acid) surfactant on the HA morphology, higher magnifications for the samples from Tests 7 and 8 are taken and given in Fig. 11. Test No. 7 was without surfactant and Test No. 8 was with 100 ppm surfactant. It was found that surfactant helps in the formation of agglomerated nanospheres. On the other hand, without surfactant, clusters from nanorods, nano tabular crystals, and nano rectangular crystals are formed. These crystals after sintering and pressing gave low hardness.

Fig. 12 shows the TEM image of the crystallized hydroxyapatite powder sample (Tests 8). It is clear that the crystallized hydroxyapatite particles from Test 8 have 30 – 80 nm size spherical shape particles. These particles are agglomerated to nanospheres with further agglomeration to micron spheres as shown from SEM.

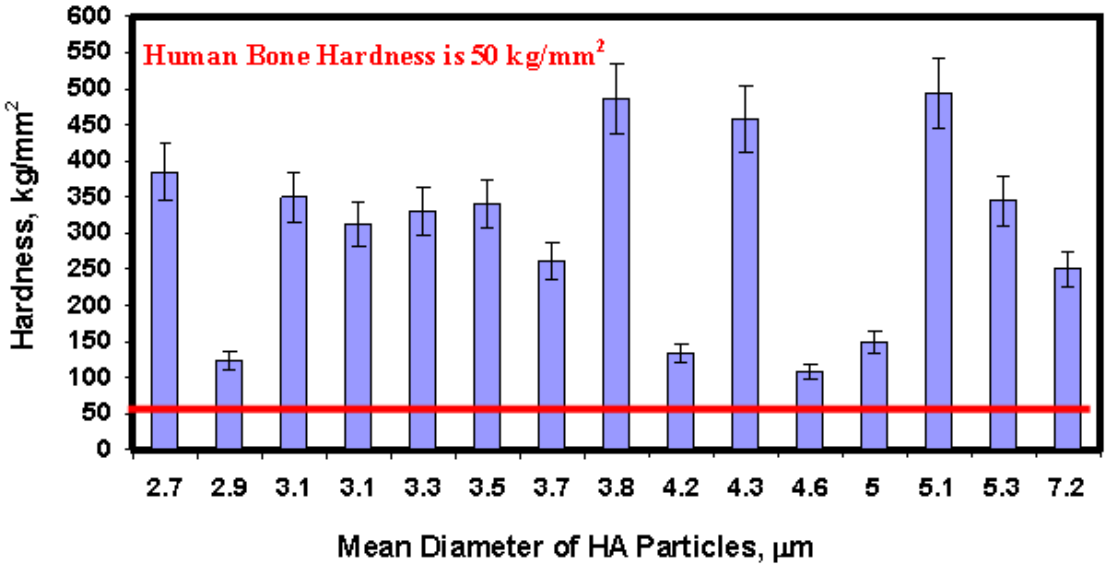

Fig. 8 No Correlation between Hydroxyapatite Hardness and Mean Diameter.

3.7. Mechanism of hydroxyapatite precipitation and its morphology modification

Precipitation of hydroxyapatite is a very rapid crystallization. Crystallization is the result of three consequent stages: supersaturation, nucleation, and crystal growth [27]. The supersaturation stage occurs when the solution contains ordered aggregates of particles (clusters) of various sizes. The nucleus will grow in size after an aggregate exceeds the critical nucleus size [32]. So, supersaturation is essential for any crystallization because crystal nucleation must start from supersaturation. The pH of the solution was adjusted to 9 ± 0.1. It was reported that alkali treatment can convert brushite and tricalcium phosphate into hydroxyapatite [18 - 22]. Fig. 13 shows the distribution of phosphate species at the hydrothermal temperature used (140 °C). It is clear that at pH 9, the predominant phosphate species is HPO_4^{2-} while PO_4^{3-} ions start to increase at pH 10. 50

IJMTI vol. 2, issue 1 (2022) 35-50 https://doi.org/ 10.21608/ijmti.2022.115060.1044

% HPO_4^{2-} ions with 50 % PO_4^{3-} ions distribution is occurred at pH = 12.128. Almost similar results were reported in another paper [7] despite different reactants and conditions being applied for the synthesis of HA.

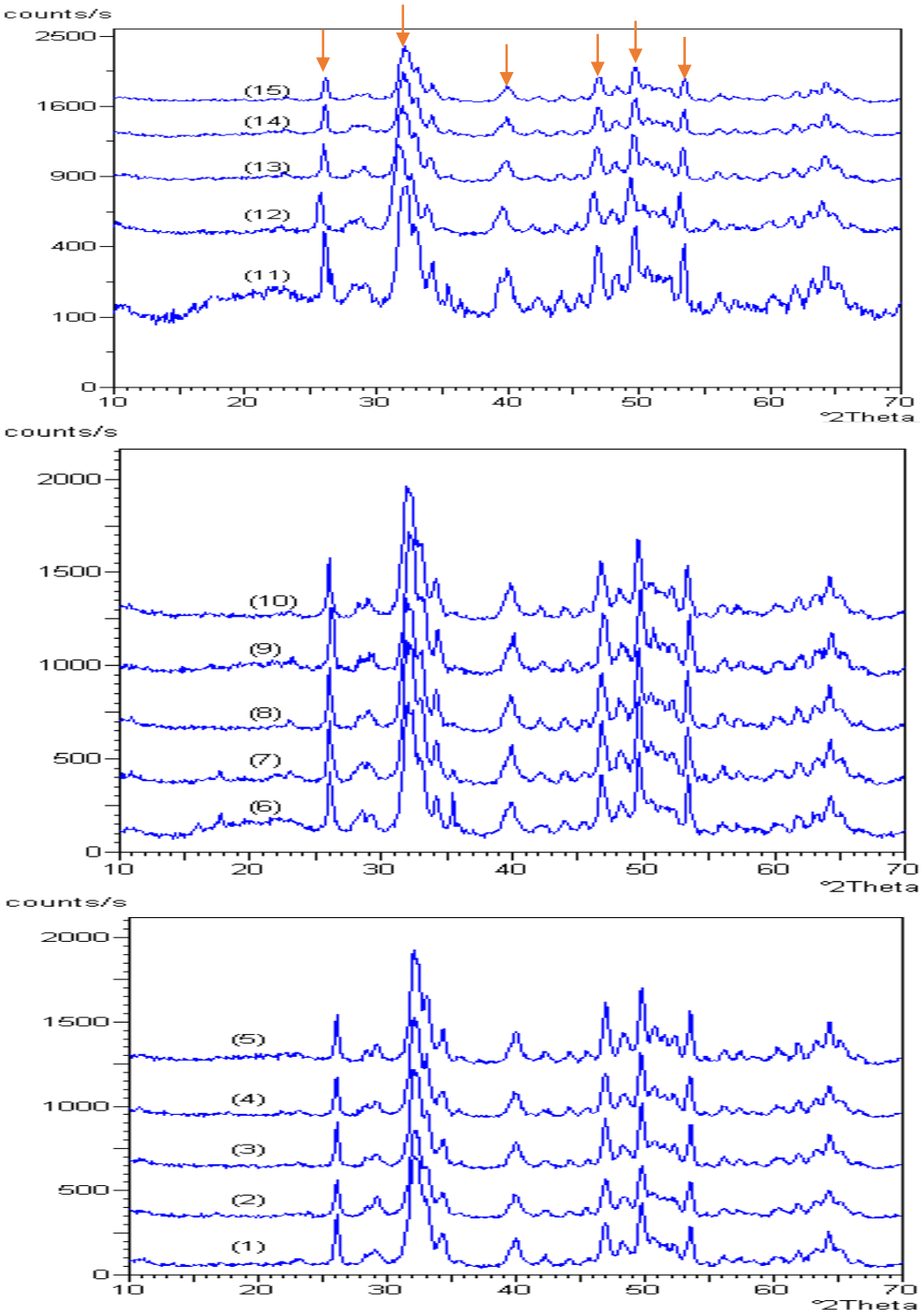

Fig. 9 XRD Pattern (XRD) of Crystallized HA Powder(15Samples)[↓HA Peaks].

IJMTI vol. 2, issue 1 (2022) 35-50 https://doi.org/ 10.21608/ijmti.2022.115060.1044

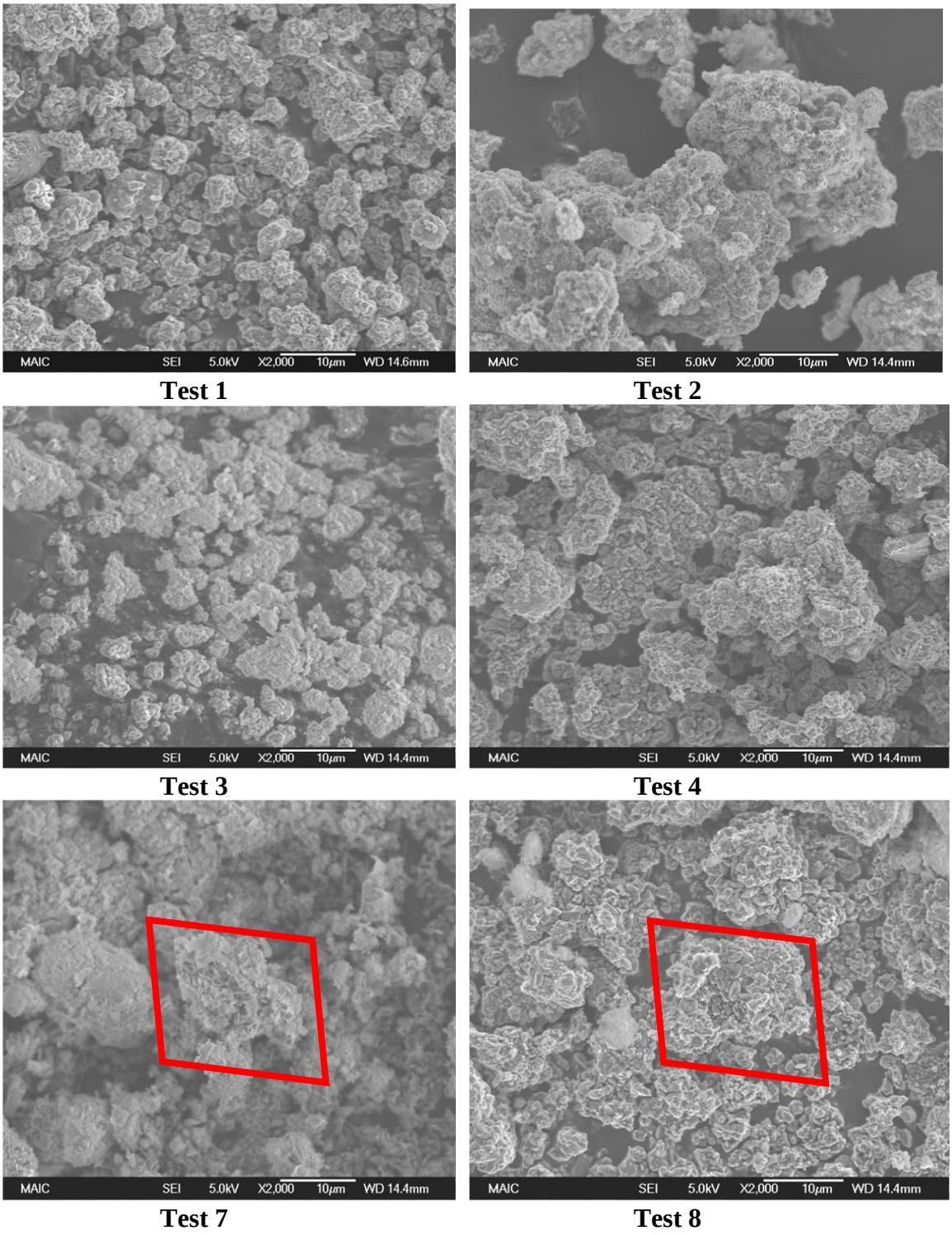

Fig. 10 SEM of Crystallized Hydroxyapatite Powder (Magnification X2000).

IJMTI vol. 2, issue 1 (2022) 35-50 https://doi.org/ 10.21608/ijmti.2022.115060.1044

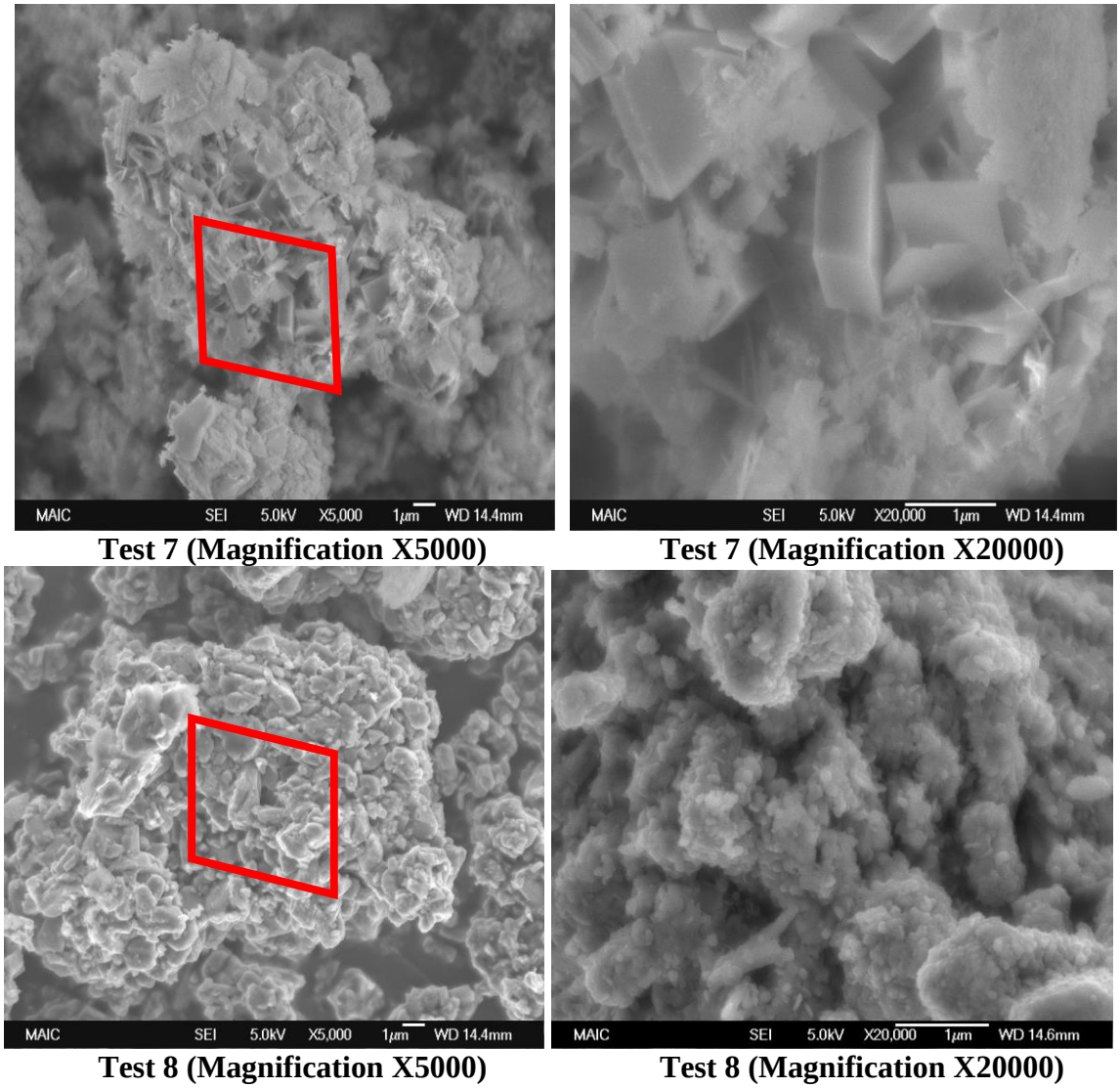

Test 7 (Magnification X5000) **Test 7 (Magnification X20000)**

Test 8 (Magnification X5000) **Test 8 (Magnification X20000)**

Fig. 11 SEM of Crystallized Hydroxyapatite Powder at Different Magnification.

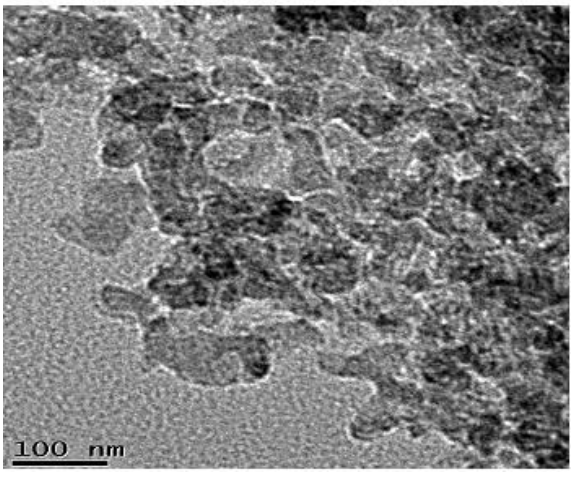

Fig. 12 TEM of Crystallized Hydroxyapatite Powder (Test 8).

Regarding the chemicals used here, the solubility of calcium acetate is 34.7 g/100 mL of water. Calcium acetate, phosphoric acid, and water are mixed. The initial pH of the mixture is ranged from 2.4 to 3.4. Then, the pH of the mixture is adjusted by ammonium hydroxide to pH 9 ± 0.1.

The effect of amino tris(methylenephosphonic acid) [ATMP] additive on hydroxyapatite crystal modification is attributed to sequestering (chelating of calcium ions). This leads to the agglomeration of fine aggregate (Fig. 11). However, without surfactant, well crystals (Tabular, Rod, and Cubic) are formed (Fig. 11). ATMP is a water-soluble (61 g/ 100 mL). In solution, it is partially hydrolyzed to anions with hydrophilic group (phosphonic groups and their counter ions). The phosphonic groups in the molecular

chain have a strong tendency to attract positively charged ions or to be attached on positively charged surfaces. Therefore, the influences of ATMP on the agglomeration of nano aggregates could be attributed to two aspects:

The negative phosphonic groups can chelate strongly the Ca^{2+} in the solution, and then decrease the supersaturation by enhancing agglomeration rather than the formation of small nuclei. So, ATMP prevents scale formation in water systems.

On the other hand, the negative phosphonic groups can be attached to the positive crystal faces of HA. It is reported that hydroxyapatite has two different types of sites, called the P and C sites, in the crystal surface of the primitive unit cell. P sites (on the (a, b) crystal face) lack calcium ions or positive charge, and C sites (on the (a, c) or (b, c) crystal face) are rich in calcium ions or positive charge [33-38]. Therefore, the negatively charged phosphonic groups will be preferentially adsorbed onto the (a, c) or (b, c) crystal faces, namely, *{*100*}* and *{*010*}* facets of the nuclei, leading to modify the nucleation and crystal growth process of HA crystals.

As mentioned above, in the absence of ATMP, HA crystals grow naturally in the presence of enough free Ca^{2+} ions in the solution. This means crystallization at a high supersaturation ratio, so high growth of tabular, rod, and cubic crystals are formed.

Chelating assisted hydrothermal synthesis of hydroxyapatite has been highly successful in obtaining agglomerated HA nanospheres. Surfactant poses the unique ability to regulate the agglomeration of hydroxyapatite particles. These particles after pressing and sintering gave high hardness compared to tabular, rod, and cubic crystals formed without surfactant.

4. Conclusion

Based on the results of the 15 hydrothermal treatment tests, it appears that the addition of amino tris(methylenephosphonic acid) $[N(CH_2PO_3H_2)_3]$ (ATMP) surfactant helps for the formation of agglomerated hydroxyapatite particles with high hardness. Synthesis in the absence of surfactant resulted in the formation of hydroxyapatite of rod-like or tabular or cubic crystals. Therefore, at alkaline pH of 9.0, the surfactant does not affect the HA mean diameter but it increases the hardness significantly. Statistical experimental design analysis indicates that increasing the concentration of reactants led to the formation of large hydroxyapatite particles. The agglomerated hydroxyapatite particles are formed from agglomerated nanospheres of hydroxyapatite. Nanospheres hydroxyapatite was formed for the tests with a surfactant at different levels of reactant concentrations and hydrothermal times. HA particle sizes ranged from 2.7 µm to 7.2 µm, whereas the crystallite sizes ranged from 26 nm to 38 nm.

Acknowledgments

The authors would like to thank the Academy of Scientific Research and Technology for funding the project entitled "Localization Hydroxyapatite Coating Technology of Medical Implants in Egypt." The Principal Investigator is Prof. Dr. Emad M. Ewais. Also, the authors would like to thank Dr. Dong-Yang Lin from the Department of Materials Science and Engineering, Zhejiang University, Hangzhou, China for drawing Fig. 13 using the computer program PHREEQC (Parkhurst and Appelo, 1999).

References

[1] J. K. Gong, J. S. Arnold, S. H. Cohn; Composition of trabecular and cortical bone, Anatomical Record (1964) 149 (3), p 325-331.

[2] L.L. Hench; "Bioceramics: From Concept to Clinic", J. Am. Ceram. Soc. 74, 7, (1991) 1487.

[3] K. Ioku, S. Yamauchi, H. Fujimori, S. Goto, and M. Yoshimura; "Hydrothermal Preparation of Fibrous Apatite and Apatite Sheet," Solid State Ionics, 151, (2002) 147.

[4] A. Cuneyt Tas; " Molten Salt Synthesis of Calcium Hydroxyapatite Whiskers," J. of Am. Ceram. Soc. 84, 2, (2001) 295.

[5] F. Branda, A. Costantini, G. Luciani, F. Rosso, G. Peluso and A. Barbarisi; "Hydroxyapatite Coating of Polyelectrolite Hydrogels by Means of the Biomimetic Method," Materials Science & Engineering, C 23, (2003) 376.

[6] J. Liu, X. Ye, H. Wang, M. Zhu, B. Wang, H. Yan, The influence of pH and temperature on the morphology of hydroxyapatite synthesized by hydrothermal method, Ceramics International 121 (2002) 59.

[7] E.A. Abdel-Aal, R. Dawood, E.M. Ewais1, W.A. Kandeel, M.A. Shemis, H.M. Abdel-Ghafar; Synthesis of Agglomerated Nano Spheres Hydroxyapatite Particles with Performance as Anti-Viral Material, International Journal of Materials Technology & Innovation (IJMTI), Vol. 1 (2021) 1-17, https://doi.org/10.21608/ijmti.2021.181066

[8] R. Ramachandra Rao, H.N. Roopa, T.S. Kannan, Solid State synthesis and thermal stability of HAp and Hap-_-TCP composite ceramic powders, Journal of Materials Science-Materials in Medicine 8 (1997) 511.
[9] P. Wang, C. Li, H. Gong, X. Jiang, H. Wang, K. Li; Effects of synthesis conditions on the morphology of hydroxyapatite nanoparticles produced by wet chemical process, Powder Technology 23, 2, (2010) 315.
[10] A. Afshar, M. Ghorbani, N. Ehsani, M.R. Saeri, C.C. Sorrell; Some important Factors in the wet precipitation process of hydroxyapatite, Materials and Design 24 (2003) 197.
[11] E.I. Dorozhkina, S.V. Dorozhkin; Application of the turbidity measurements to study in situ crystallization of calcium phosphates, Colloids and Surfaces 203 (2002) 237.
[12] G. Bezzi, G. Celotti, E. Landi, T.M.G. La Torretta, I. Sopyan, A. Tampieri; A novel sol–gel technique for hydroxyapatite preparation, Materials Chemistry and Physics 78 (2003) 816.
[13] W. Weng, G. Han, P. Du, G. Shen; The effect of citric acid addition on the formation of sol–gel derived hydroxyapatite, Materials Chemistry and Physics 74 (2002) 92.
[14] K. Yamashita, T. Arashi, K. Kitagaki, S. Yamada, T. Umegaki; Preparation of apatite thin films through sputtering fromcalcium phosphate glasses, Journal of American Ceramic Society 77, 9, (1994) 2401.
[15] C.C. Silva, A.G. Pinheiro, M.A.R. Miranda, J.C. Go´es, A.S.B. Sombra; Structural properties of hydroxyapatite obtained by mechanosynthesis, Solid State Sciences 5 (2003) 553.
[16] S. Nakamura, T. Isobe, M. Senna; Hydroxyapatite nano sol prepared via a mechanochemical route, Journal of Nanoparticle Research 3 (2001) 57.
[17] E.A. Abdel-Aal, A.A. El-Midany, and H. El-Shall, Mechanochemical-Hydrothermal Preparation of Nano-crystallite Hydroxyapatite Using Statistical Design, Materials Chemistry and Physics 112 (2008) 202.
[18] E.A. Abdel-Aal, D. Dietrich, S. Steinhäuser, T. Lampke; Strontium-substituted Hydroxyapatite Coatings on Titanium by Electrodeposition Technique, Journal for Electrochemistry and Plating Technology, 3 (2011) 29, ISSN 1866-7406.
[19] E.A. Abdel-Aal, D. Dietrich, S. Steinhaeuser, B. Wielage; Electrocrystallization of Calcium Phosphate Coatings on Titanium Substrate at Different Current Densities, Surface and Coating Technology 202 (2008), 5895.
[20] E.A. Abdel-Aal; Inserting of Strontium During Coating of Hydroxyapatite, International Journal of Nanoparticles, Vol. 4, No. 1, (2011), 77.
[21] E.A. Abdel-Aal; Electrodeposition of Calcium Phosphate Coatings on Titanium Alloy Implant at Different Ca/P Ratios and Different Times, International Journal of Nano and Biomaterials, Vol. 3, No. 2, (2010), 187.
[22] E.A. Abdel-Aal, D. El-Sayed, M. Shoeib, A.T. Kandil, Enhancing Coating of Brushite/hydroxyapatite Layer on Titanium Alloy Implant Surface with Additives, Applied Surface Science, Part B, 285 (2013), p. 136-143.
[23] G.K. Lim, J.Wang, S.C. Ng, C.H. Chew, L.M. Gan; Processing of hydroxyapatite via microemulsion and emulsion routes, Biomaterials 18 (1997) 1433.
[24] E.A. Abdel-Aal, S.M. Malekzadeh, M.M. Rashad, A.A. El-Midany, H. El-Shall; Effect of synthesis conditions on preparation of nickel metal nanopowders via hydrothermal reduction technique, Powder Technology 171 (2007) 63-68.
[25] A.A. Ismail, A. El-Midany, E.A. Abdel-Aal, H. El-Shall; Application of Statistical Design to Optimize the Preparation of ZnO Nanoparticles via Hydrothermal Technique, Materials Letters 59 (2005) 1924-1928.
[26] X. Xiao, R. Liu, F. Liu, X. Zheng, D. Zhu; Effect of poly(sodium 4-styrene-sulfonate) on the crystal growth of hydroxyapatite prepared by hydrothermal method, Materials Chemistry and Physics 120 (2010) 603.
[27] H. Zhang, B. W. Darvell; Synthesis and characterization of hydroxyapatite whiskers by hydrothermal homogeneous precipitation using acetamide, Acta Biomaterialia 6 (2010) 3216.
[28] H. El-Shall, M.M. Rashad, and E.A. Abdel-Aal; "Effect of Phosphonate Additive on Crystallization of Gypsum in Phosphoric and Sulfuric Acid Medium," Crystal Research Technology, 37, (2002) 1264.
[29] L. Yan, Y. Li, Z. X. Deng, J. Zhuang, and X. Sun; "Surfactant-Assisted Hydrothermal Synthesis of Hydroxyapatite Nanorods," International Journal of Inorganic Materials, 3, (2001) 633.
[30] G. Muralitharn, and S. Ramesh; The Effects of Sintering Temperature on the Properties of Hydroxyapatite, Ceramics International, 26, (2002) 221.

IJMTI vol. 2, issue 1 (2022) 35-50 https://doi.org/ 10.21608/ijmti.2022.115060.1044

[31] M. Ramrakhiani, P. Deepti and T.S. Murty; Micro-Indentation Hardness Studies on Human Bones, Acta Anatomica, 103, (1979) 358.
[32] H. Zhang, Y. Wang, Y. Yan and S. Li; "Precipitation of Biocompatible Hydroxyapatite Whiskers From Moderately Acid Solution," Ceramics International, 29, (2003) 413.
[33] M.M. Rashad, M.H.H. Mahmoud, I.A. Ibrahim and E. A. Abdel-Aal, Effect of Citric Acid and 1,2- Dihydroxybenzene 3,5-disulfonic Acid on Crystallization of Calcium Sulfate Dihydrate Under Simulated Conditions of Phosphoric Acid Production, Crystal Research and Technology 40, 8 (2005), p. 741-747.
[34] E. A. Abdel-Aal, H. M. Abdel-Ghafar, and M. B. El Anadouli; New Findings About Nucleation and Crystal Growth of Reverse Osmosis Desalination Scales with and without Inhibitor, Crystal Growth & Design 15, 10 (2015), p. 5133-5137.
[35] H. El-Shall, M. M. Rashad, and E. A. Abdel-Aal; Effect of Cetyl Pyridinium Additive on Crystallization of Gypsum in Phosphoric and Sulfuric Acids Medium, Crystal Research and Technology 40, 9 (2005), p. 860-866.
[36] H. El-Shall, E. A. Abdel-Aal and B. Moudgil, Cost-Effective Reagents as Defoamers and Crystal Modifiers to Enhance the Filtration of Phosphogypsum, Publication No. 01-141-162, Florida Industrial and Phosphate Research Institute (FIPR) Project No. 96-01-141, Florida University, USA, (1999), p. 1-63, https://fipr.floridapoly.edu/
[37] H. El-Shall, E. A. Abdel-Aal and B. Moudgil, Effect of Surfactants on Phosphogypsum Crystallization and Filtration during Wet-Process Phosphoric Acid Production, Separation Science and Technology Journal, 35, 3 (2000), p. 395-410.
[38] E.A. Abdel-Aal, M.H.H. Mahmoud, H. El-Shall, A.K. Ismail, Increasing the filtration rate of phospho-gypsum using surfactant, Hydrometallurgy, 85 (2007), p. 53-58.